INDUSTRIAL AND BIOMEDICAL APPLICATIONS

Frank Smith, Nicholas Ovenden and Richard Purvis

University College London, Mathematics Department, UCL, Gower St, London WC1E 6BT
tel. (UK) 02076792839, fax (UK) 02073835519, email frank@math.ucl.ac.uk

Abstract: Theoretical models for two distinct current applications are described, one industrial on violent water-air interaction during an impact process and the other biomedical on network flow. Each involves Prandtl's boundary-layer equations, accompanied by very short-scale physical adjustments. Oblique impacts and successive bifurcations are the respective particular themes.

Key words: industrial, biomedical, impacts, networks, theory, computation, scales.

1. INTRODUCTION

It is a pleasure to pay tribute to the great leader and innovator Ludwig Prandtl. What an inspiration he and his work were and still are!

A common feature in the two areas of modelling described in the present article is the laminar boundary layer for an incompressible fluid. Among Prandtl's many other brilliant researches, his idea of the *Grenzschicht* (boundary layer) and related thin viscous layers led to the flowering of singular perturbation studies and multiple scaling in engineering and mathematics during the twentieth century and their continuation into the twenty-first. The idea has had enormous application in industry over decades, not only in aeronautics but in many other fields as well. More recently the application in biomedical studies has grown.

We focus on two distinct applications from recent work, one industrial on violent water-air interaction during an impact process and

the other biomedical on networks. Background work on the former is described fully in [**1-7**] and on the latter in [**8-14**]. Since the flow in each case is very difficult to solve in full by direct computation, the present new contribution uses the Prandtl idea of thin viscous layers, among several other features, to help improve physical understanding and to create predictions and comparisons.

Sections 2, 3 describe the industrial and the biomedical applications in turn, highlighting the short-scale physical changes which are another common feature. In each application Prandtl's boundary-layer equations,

$$u_x + v_y = 0, \tag{1.1a}$$

$$u_t + u\, u_x + v\, u_y = -\, p_x\,(x, t) + Re^{-1}\, u_{yy} \tag{1.1b}$$

play a key role in the thin layers present. The equations are written here in non-dimensional form with velocity field (u, v) in respective Cartesian coordinates (x, y), pressure p and time t. In the usual manner, the relevant dimensional scalings are a typical flow speed U*, a representative length L and the fluid density ρ. The Reynolds number Re is U*L/ν, with ν denoting kinematic viscosity, and planar motion is assumed. Section 4 provides final comments.

2. IMPACTS: OBLIQUENESS AND AIR EFFECTS

A main issue in impacts concerns when and how substantial air-water interaction first occurs near the oblique impact of a water droplet onto a flat horizontal fixed solid surface (wall) or another body of water, with air in-between, as in Fig. 1. The effects of an oblique approach can be significant in industrial terms and so these are incorporated whereas other important effects such as from gravity, surface tension and compressibility are examined in the literature cited in the previous section. The representative quantities U*, L here are taken to be the vertical component V of the droplet approach velocity and a typical droplet diameter, while ρ is ρ_1 , the density of the water (or fluid 1), likewise ν is ν_1 in the water, and the pressure is measured relative to the atmospheric value. The coordinates and time are centred near the area and instant of impact. The starting point is the Navier-Stokes equations, which are, with Δ denoting the Laplacian,

$$\underline{u}_t + (\underline{u}\ .\ \text{grad})\ \underline{u} = -\,(\rho_1 / \rho_n)\ \text{grad}\ p + (\nu_n / \nu_1)\ Re^{-1}\ \Delta\underline{u} \tag{2.1}$$

both in the water, with subscript n = 1, and in the air (fluid 2) with n = 2 where the air density and kinematic viscosity are ρ_2, ν_2 in turn. The continuity equation (1.1a) applies in each fluid. The impact then has rapid local interaction involving the thin air layer.

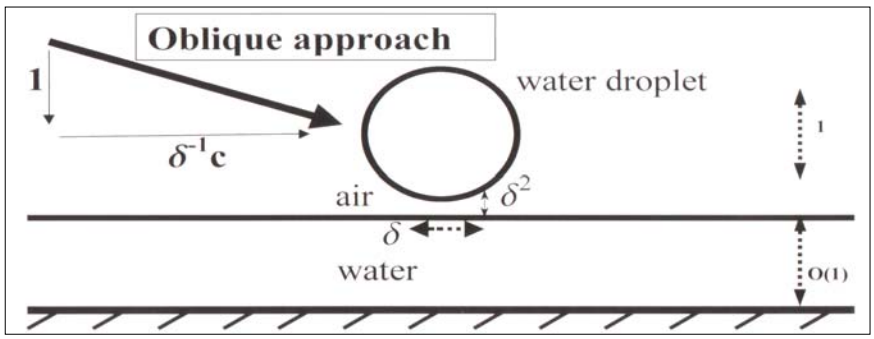

Figure 1. Diagram of oblique impact involving water droplet, air and water/solid surface.

The present theory now takes the density and viscosity ratios ρ_2 / ρ_1, μ_2 / μ_1 of the two fluids 1, 2 to be small: for dry air with pure water these two ratios are near 1/828 and 1/55 in turn, at 20 degrees C and one-atmosphere pressure. Near impact, as the aspect ratio δ of the air layer becomes small, the length scalings of that layer are $(x, y) = (\delta X, \delta^2 y_2)$ in view of the droplet's O(1) curvature, whereas the length scalings in the water are $(\delta X, \delta Y)$. An order of magnitude argument therefore suggests

$$(u, v, p) = (\delta^{-1}c + u_1, v_1, \delta^{-1}p_1) + \ldots \text{ in the water,} \qquad (2.2a)$$

$$(u, v, p) = (\delta^{-1}u_2, v_2, \delta^{-1}p_2) + \ldots \text{ in the air} \qquad (2.2b)$$

based on the kinematic and pressure conditions at the unknown interface and on (1.1a), (2.1), with the typical time scale $t = \delta^2 T$ being short. The size $\delta^{-1}c$ of the relative incident horizontal velocity component U/V (see also Fig. 1) of the droplet is such as to significantly affect the local interaction. The governing equations in the air are of thin-layer type. In fact the individual contributions in (2.1) for n = 2 are now of order δ^{-3} [acceleration], δ^{-3} [inertia], δ^{-2} (ρ_1 / ρ_2) [pressure gradient], (ν_2 / ν_1) Re^{-1} δ^{-5} [viscous] in the x direction and all are in balance if $Re \sim (\nu_2 / \nu_1)\ \delta^{-2}$ and $(\rho_2 / \rho_1) \sim \delta$, yielding

$$Re \sim (\nu_2 \rho_1^{\,2}) / (\nu_1 \rho_2^{\,2}) \,. \qquad (2.3)$$

Hence the air-water interaction is controlled by the coupled system of (1.1a, b) in the air, provided (X, y_2, T, 1, u_2, v_2, P) replaces (x, y, t, Re, u, v, p), along with

$$(\partial_T + c\,\partial_x)^2 F = \pi^{-1}\,(P.V.)\int P_s(s, T)\,(X-s)^{-1}\,ds \qquad (2.4)$$

from the unsteady potential flow in the water, where the principal value integral extends from minus infinity to plus infinity. The unknown pressure P stands for p_1 evaluated at Y zero and is identical to p_2. The boundary conditions on (1.1a, b) include the kinematic condition on v_2 and a matching constraint $u_2 = c$ at the unknown scaled interface $y_2 = F$, as well as no slip at y_2 zero.

The estimate (2.3) acts as a critical Reynolds number and its value is about 10^7 for water with air. Because of the industrial setting [**1, 4-7**] where typical Re values of 10^4 to 10^5 are encountered there is much interest in the subcritical range. There (1.1a, b) and the appropriate boundary conditions reduce to the Reynolds lubrication equation

$$(F^3 P_X)_X = 12\,(F_T + c\,F_X/2) \qquad (2.5)$$

in normalised form. So far the working is for oblique droplet impact onto a fixed solid but essentially the same system (2.4), (2.5) applies for impact onto water [**5, 7**]. Also, equivalent equations hold in a frame moving with the horizontal velocity U of the droplet where the wall appears as an upstream-moving wall [**7**].

Computational solutions of (2.4), (2.5) were obtained by adapting a numerical method from the papers [**5, 7**], which address the case of zero c (normal impact). Grids and time steps similar to those used in these papers were applied here as well and tested satisfactorily for accuracy. The initial conditions and the far-field boundary conditions are those of an approaching parabola shape $(X-cT)^2 - T$ for F, corresponding to the lower reaches of the smooth total incoming droplet, and of negligible induced pressure (P tending to zero) which is associated with the atmospheric pressure holding outside the interaction region. The results for two different positive values of c are shown in Fig. 2 and indicate effects not dissimilar to those of inclined gravity [**7**]. A skewed touchdown (F tending to zero) is indicated generally at negative T; thus the presence of air hastens touchdown. This is in the fixed frame, note, with a relatively high incident horizontal velocity component, and the angle of approach measured from the horizontal is V/U, i.e. δ / c. In the extreme of large c the majority of the solution has $T \propto c$ and enlarged lengths $X-cT \propto c^{1/2}$, so that in a moving frame the right side of (2.5)

approaches -6c F_X ; (2.5) now integrates to give F^3 P_X as -6c F + G(T). Here G must be nonzero to give zero farfield P. Substitution into (2.4) to yield an F equation then suggests that the G term drives the touchdown process, in which the minimum F tends to zero in a square-root manner in scaled time.

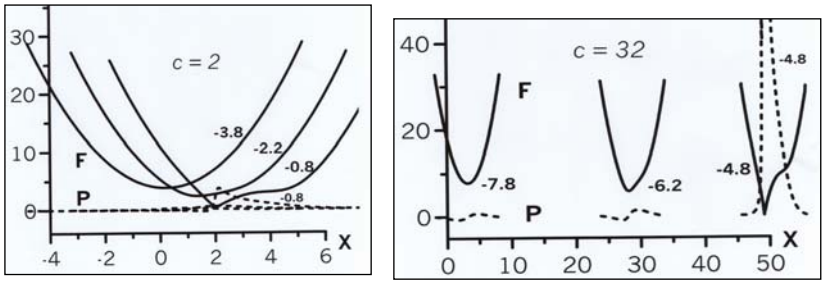

Figure 2. Droplet shapes (solid) and pressures (dashed) for two c values, at times marked.

More widely, the results also prompt thoughts on pre-existing air flow effects since we would expect such air flow also to provoke skewing, for example by means of an extra streamwise mass flux. Analysis for large negative T however suggests that, at least for zero c, skewing is present only if the incident shape is already skewed. This is because the farfield P must be zero. Solutions with such incident skewing are included in [**7**]. With nonzero c an extra mass flux is induced but it is a definite amount rather than arbitrary. In fact, skewing of the incident shape may well be how pre-existing air flow influences the impact process in practice, by altering the droplet shape considerably before the local interaction comes into play.

3. NETWORK FLOW

Moving on to the separate issue of networks, we describe modelling of a planar network of bifurcating tubes as in Fig. 3 starting at x = 0. The representative quantities U*, L here are, respectively, a typical axial speed induced in the incident mother flow (taken to be fully developed motion with no slip at the walls and unknown total mass flux) and a typical tube width. Steady flow is assumed over a long length scale that is nevertheless short compared with the viscous length Re, together with zero pressure upstream in the mother and prescribed pressures at the

downstream ends of the network. The upstream-influence length scale axially [**11**] is O (ϵ^{-1}) where ϵ^7 is 1/Re and is small. The thin viscous layer at the lower outer wall near y = 0 then has thickness of order ϵ^2 and Prandtl's equations (1.1a, b) hold there in re-scaled terms with Re replaced by unity. The boundary conditions required are

$$u \sim \lambda_0 (y + A (x)) \qquad \text{as } y \rightarrow \infty, \tag{3.1a}$$

$$\text{no slip at } y = f (x), \tag{3.1b}$$

where the positive constant λ_0 stands for the scaled incident wall shear and f(x) denotes the given lower-wall shape. If we ignore upstream influence for now, the negative boundary-layer displacement A(x) can be obtained (to within a factor related to the mass flux) by the core-flow solution valid outside the wall layer; see below. In that case the viscous wall-layer problem determines the ϵ^4 scaled wall pressure p to within a constant.

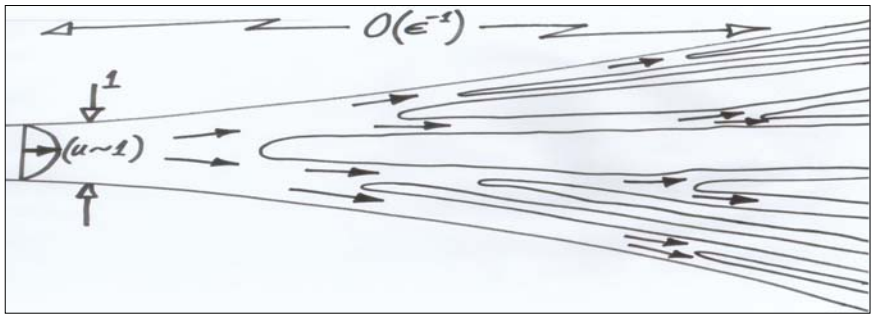

Figure 3. Schematic of a branching network with successive bifurcations

Suppose first that we have a single 1-to-2 branching. The inviscid core then within the lower daughter acts mostly as if distinct from that in the upper daughter and likewise for the viscous upper wall layer, over the present length scales. In the lower daughter core, the pressure is of order ϵ^4 and the stream-function expands as

$$\psi = \psi_0 (y) + \epsilon^2 \{ A (x) u_0 (y) + \lambda_2 \psi_0 (y) \} + \ldots \tag{3.2}$$

where ψ_0 is $\lambda_0 (y^2 / 2 - y^3 / 3)$ and u_0 is $\lambda_0 (y - y^2)$, corresponding to the fully developed Poiseuille flow in the absence of any bifurcation, whereas the constant λ_2 is an unknown associated with the altered mass flux. The undeveloped viscous layers on the internal dividers of the daughters have negligible impact on the flow (they are passive), implying a tangential flow condition on the given divider underside $y = c_0 - \epsilon^2$

$T_0(x)$ say. Taking $T_0(0)$ as zero without loss of generality thus yields the classical thin-channel result

$$A(x) = T_0(x) + K_0, \quad \text{for } x > 0, \tag{3.3}$$

(since $u_0(c_0)$ is nonzero) which determines the function $A(x)$ to within the additive constant K_0. Similarly, upstream influence present in the mother tube yields a free-interaction behaviour [**11**]

$$A(x) = K e^{\kappa x}, \quad \text{for } x < 0, \tag{3.4}$$

where κ is a known positive constant and (3.4) represents an elliptic effect. A novel feature due to the presence of the bifurcation (branching junction) however is that an axial jump in displacement can occur across the daughter entrances from 0- to 0+. The jump is admissible, and in fact necessary due to the set pressures upstream and downstream [**12, 14**]. At the outer walls in particular, where the incident velocity is close to zero, the viscous layers of (3.1a,b) allow the Bernoulli quantity $p + u^2/2$ to be conserved as required along each local inviscid streamline by means of a scaled pressure jump, in this case $\lambda_0^2 (K^2 - K_0^2)/2$. The jumps are smoothed out over a shorter axial scale by an Euler region of length O(1) in x [**12-14**], which provides some direct communication between the two daughters and the mother. The feature that K, K_0 are unequal in general allows adjustment of K_0 in order to allow the lower-daughter pressure to satisfy the downstream pressure conditions, and likewise for the upper daughter.

Second, suppose a 1-to 4 network. Then another new feature appears as follows. Again attention can be restricted to a lower part, consisting now of a daughter described essentially as in (3.2) and two granddaughters which begin at $x = x_1 > 0$. The lower of these granddaughters is also described essentially by (3.2). The upper one however must suffer higher typical pressure variations of order ϵ^2 such that

$$\psi = \psi_0(y) + \epsilon^2 \{ D(x) u_0(y) + \lambda_2 [\psi_0(y) - \psi_0(c_1)] \} + \ldots \tag{3.5}$$

where $c_1 - \epsilon^2 T_1(x)$, $c_1 + \epsilon^2 S_1(x)$ are the underside and topside respectively of the divider between these two granddaughters and

$$D(x) = - p_1(x) \int u_0^{-2}\, dy - S_1(x) + \gamma_1 . \tag{3.6}$$

The integral is from c_1 to y, while the ϵ^2 scaled pressure p_1 and the constant γ_1 are unknown. The novel feature here is that another jump must usually occur, namely in pressure across the entrance of the upper granddaughter from x_1- to x_1+. This again is admissible, as the incident velocity is nonzero at all y heights of that granddaughter, allowing the Bernoulli property to be maintained along each streamline. This active jump is also smoothed out on a shorter axial scale by an O(1) Euler region in $x - x_1$. (Overall this is another type of ellipticity.) As a result, it is found that a jump is also induced in the effective A(x) function here which although still similar to (3.3), (3.4) now has

$$A(x) = K e^{\kappa x}, \text{ (discontinuity), } T_0(x) + K_0, \text{ (discontinuity), } T_1(x) + K_1 \quad (3.7)$$

The doubly discontinuous form (3.7) then drives the viscous wall-layer response by means of the constraint (3.1a). The displacement constants K_0, K_1 in (3.7) are controlled not only by the outermost (lower granddaughter) imposed pressure downstream but also by the inner (upper) granddaughter pressure imposed downstream.

Third, suppose a 1-to-8 network. Again consider its lower part. Yet another new feature enters as this new generation can contain some inner bifurcations which have nonzero incident velocity throughout and so can provoke the higher $O(\epsilon^2)$ pressure (and jumps) all the way across in y as well as for long distances axially upstream and downstream, while outermost bifurcations continue the earlier established trend. One case, to focus attention, has the triply discontinuous form

$$A(x) = \text{as in (3.7), then a discontinuity, then } T_2(x) + K_2 \ . \quad (3.8)$$

The three constants K_0, K_1, K_2 however depend on the four pressures imposed downsteam in the four great-granddaughters (of this lower part) via the higher pressure responses and pressure jump occurring in the (implied) inner bifurcation as just described. The forms alternative to (3.8) in a 1-to-8 network depend on the relative positioning of each divider, making either (3.7) or a four-times discontinuous form hold.

Larger/generalized networks produce similar effects, i.e. potentially many discontinuities in the negative displacement A(x) which, along with f(x), forces the viscous layer by means of (3.1a,b) and induces discontinuities in the wall pressure(s). The viscous layer is nonlinear in general, requiring numerical solution and admitting separation [**11-14**]. By virtue of Prandtl's transposition theorem, the solution depends only on the effective thickness (A+f) [=B say], thus giving wide application.

For small B, a linearized form applies and gives merely small discontinuities in pressure as in Fig. 4. The sample solutions in Fig. 4 show the scaled pressure induced at an outer wall: the "1 or 5 branchings" refers to the number of branching junctions as seen from that outer wall only, whereas the total system could have more branching junctions unseen from that wall (as in Fig. 3 for example). A contraction of the outermost tube width broadly leads to a favourable pressure gradient and increasing wall shear, and expansion to an adverse pressure gradient with decreasing wall shear, as expected, but the discontinuities due to the branching junctions can counteract those trends.

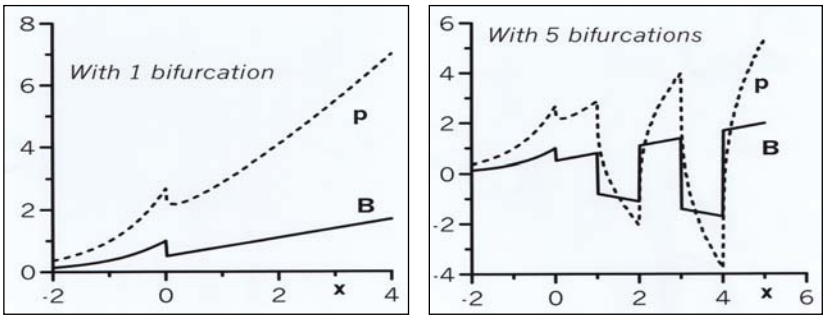

Figure 4. Outer-wall pressure in networks with 1 or 5 seen branchings, for effective thicknesses B as shown. The seen junctions are at x = 0 (left) and 0, 1, 2, 3, 4 (right).

4. FURTHER COMMENTS

Concerning the industrial application in section 2, an extension akin to the extreme for large c might admit an account of skimming (bouncing) via ground effect, an extension which is similar to using an enhanced Reynolds number based on U. Along with that, and the limit of quasi-inviscid air studied anew in [**5**], it would clearly be interesting to see what happens when the complete Prandtl system (1.1a,b) applies, even including compressibility for instance. Concerning the biomedical application in section 3, the presence of multiple jumps in the solution(s) is likewise intriguing, especially if coupled with separation in nonlinear and/or unsteady cases [**12, 14**]. Common needs for both applications are increased understanding of three-dimensional phenomena eventually, further investigation of full nonlinearity and following through on ideas from the current article, all of which is partly continuing work. We aim to report more later.

Above all, Prandtl's full boundary-layer system (1.1a,b) remains fascinating and relevant. Both extreme and linearized cases in this article exhibit the rich structure and physics arising from the system. The article

also hints clearly, we hope, at the richness and diversity in terms of application areas.

ACKNOWLEDGEMENTS

Industrial: we thank EPSRC and QinetiQ for support through the Faraday Partnership for Industrial Mathematics, managed by the Smith Institute, and also David Allwright, Roger Gent, David Hammond, Richard Moser and Manolo Quero for their interest and helpful discussions. **Biomedical:** we thank EPSRC for support through the Mathematics Programme and Life Sciences interface, and also Neil Kitchen, Stefan Brew, Joan Grieve, Robert Bowles and Stephen Baigent for their interest and helpful discussions.

REFERENCES

1. Gent RW, Dart NP, Cansdale JT. "Aircraft icing", *Phil Trans Roy Soc A*, **358**, pp. 2873-2911, 2000.
2. Josserand C, Zaleski S. "Droplet splashing on a thin liquid film", *Phys Fluids*, **15**, pp. 1650-1657, 2003.
3. Wilson SK. "A mathematical model for the initial stages of fluid impact in the presence of a cushioning fluid layer", *J Eng Maths*, **25**, pp. 265-285, 1991.
4. Purvis R, Smith FT. "Large droplet impact on water layers", *Proc. 42nd Aerospace Sci Conference*, Reno, NV, USA, Jan. 5-8, 2004, paper no. 2004-0414.
5. Purvis R, Smith FT. "Air-water interactions near droplet impact", *Euro J Applied Maths*, to appear, 2004.
6. Purvis R, Smith FT. "Droplet impact on water layers: post-impact analysis and computations", *Phil Trans Roy Soc A*, in press, 2004.
7. Smith FT, Li L, Wu G-X. "Air cushioning with a lubrication / inviscid balance", *J Fluid Mech*, **482**, pp. 291-318, 2003.
8. Brada M, Kitchen ND. "How effective is radiosurgery for arteriovenous malformations?", *J Neurol Neurosurg Psychiatry*, **68**, pp. 548-549, 2000.
9. Hademenos G.J, Massoud T.F. and Vinuela F. "A biomathematical model of intercranial arteriovenous malformations based on electric network analysis: theory and haemodynamics", *Neurosurgery*, **38**(5), pp. 1005-1015.
10. Zhao Y, Brunskill CT, Lieber BB. "Inspiratory and expiratory steady flow analysis in a model symmetrically bifurcating airway", *J Biomech Eng*, **119**, pp. 52-65, 1997.
11. Smith FT. "Upstream interactions in channel flows", *J Fluid Mech*, **79**, pp. 631-655, 1997.
12. Smith FT, Ovenden NC, Franke P, Doorly DJ. "What happens to pressure when a flow enters a side branch?", *J Fluid Mech*, **479**, pp. 231-258, 2003.
13. Smith FT, Jones MA. "AVM modelling by multi-branching tube flow: large flow rates and dual solutions", *IMA J Maths Medicine Biol*, **20**, pp. 183-204, 2003.
14. Smith FT, Dennis SCR, Jones MA, Ovenden NC, Purvis R, Tadjfar M. "Fluid flows through various branching tubes", *J Eng Maths*, **47**, pp. 277-298, 2003.